



EXPERIMENTAL STUDIES OF HIGH SEISMIC PERFORMANCE SHEAR WALLS

Wen-I Liao¹, Jianxia Zhong², C.C. Lin³, Y.L. Mo⁴ and Chin-Hsiung Loh⁵

SUMMARY

Past RC panel tests performed at the University of Houston show that reinforced concrete membrane elements under reversed cyclic loading have much greater ductility when steel bars are provided in the direction of principal tensile stress. In order to improve the ductility of low-rise shear walls under earthquake loading, high seismic performance shear walls have been proposed to have steel bars in the same direction as the principal direction of applied stresses in the critical regions of shear walls. This paper presents the test results of four large-scale shear walls, including two shear walls under shake table tests and two shear walls under reversed cyclic loading. The height, length, and width of the designed shear walls for the shake table tests are 0.7 m, 1.4 m and 0.085 m, respectively. The height, length, and width of the designed shear walls for the reversed cyclic tests are 1.4 m, 2.8 m and 0.12 m, respectively. Steel bars are provided in the directions of 45 degrees to the horizontal that are very close to the principal direction of applied tensile stresses according to the elastic analysis of the shear walls. The steel ratio in both perpendicular directions of the shear walls is 0.36% for the shake table tests, and 0.48% for the cyclic tests. For the two shear walls under dynamic loading induced by the shake table, the response time histories for the accelerations and displacements as well as the hysteretic loops are presented. For the two shear walls under reversed cyclic loading, the force-displacement hysteretic loops are presented. Based on the experimental results, the tested high performance shear walls have greater ductility than that of conventional shear walls.

Keywords: shear wall, high seismic performance, ductility factor, dissipated energy capacity.

¹ Assistant Professor, Assistant Professor, Dept. of Civil and Environmental Engineering, National University of Kaohsiung, Kaohsiung, Taiwan. Email: wiliiao@ncree.gov.tw

² Ph.D. Student, Dept. of Civil and Environmental Engineering, University of Houston, Houston, Texas, USA. Email: Jianxia.Zhong@mail.uh.edu

³ Assistant Research Fellow, National Center for Research on Earthquake Engineering, Taipei, Taiwan. Email: cclin@sun.ncree.gov.tw

⁴ Professor, Dept. of Civil and Environmental Engineering, University of Houston, Houston, Texas, USA. Email: yilungmo@egr.uh.edu

⁵ Professor and Director, National Center for Research on Earthquake Engineering, Taipei, Taiwan. Email: loh@ncree.org.tw

INTRODUCTION

Shear walls can be divided into three groups based on the ratio of height to width. When the height to width ratio is greater than 2.0, they are called high-rise shear walls; when the height to width ratio is less than 1.0, they are called low-rise shear walls; when the height to width ratio is between 1.0 and 2.0, they are called medium-rise shear walls. For high-rise shear walls, the failure is mainly governed by flexure. In contrast, for low-rise shear walls, the failure is mainly governed by shear. For medium-rise shear walls, the failure is governed by both flexure and shear.

The stiffness characteristics and shear strength of shear walls have been investigated during the 1990s (Elnashai et al. [3]; Wood [14]; Farrar and Baker [5]; Cheng et al. [1]; Colotti [2]; Eberhard and Sozen [3]). In the past 20 years, attention was given to the seismic behavior of reinforced concrete shear walls. Strength, ductility characteristic and energy dissipation aspects of shear walls under earthquake have been studied (Pilakoutas and Elnashai [11], Mo and Kuo [9]; Mo and Lee [10]; Tasnimi [13]; Lopes [6]). Test results show that conventional low-rise and mid-rise shear walls have less ductility and lower energy dissipation, which can be observed as “pinching effect” in the hysteretic response of shear walls.

The reason why conventional low-rise shear walls do not exhibit satisfactory ductility is that there is an angle between the orientations of rebars and the principal direction of applied tensile stresses on shear walls, therefore the ductility of rebars can not be fully utilized.

Recent test results conducted at the University of Houston (Mansour et al. [8]) and by Sittipunt et al. [12] show that the effect of the steel grid orientation plays an important role on the cyclic shear stress-shear strain relationships of reinforced concrete panels and walls. Both the energy dissipation capacity and ductility are greater when steel bars are in the principal direction of the applied tensile stresses.

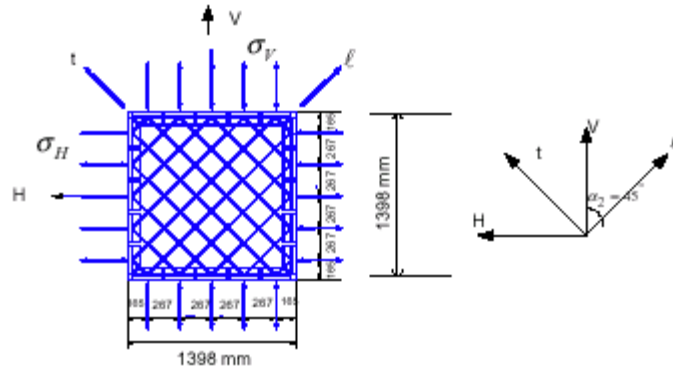
In order to improve the seismic behavior of low-rise shear walls under earthquake loading, high performance shear walls have been proposed to have steel bars in the principal direction of applied tensile stresses in the critical regions of shear walls. This paper presents the results from the shake table tests on two shear walls and from the reversed cyclic loading tests on two shear walls. It is found that the seismic performance of shear walls can significantly be improved when steel bars are provided in the principal direction of applied tensile stresses.

PREVIOUS RESEARCH

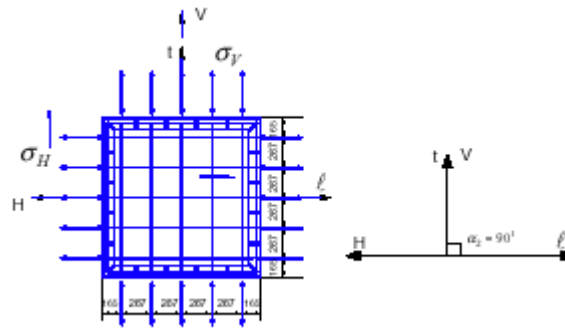
Fifteen full-size reinforced concrete membrane elements (panels) subjected to reversed cyclic stresses at the University of Houston were tested (Mansour [7]). Two series of the tests (CA and CE) are conducted to study the effect of the steel grid orientation on the cyclic shear stress - shear strain curves. In specimens of series CA, there is a 45-degree between steel grid orientation and the applied principal stresses. In series CE, the steel grid orientation is provided in the direction of the applied principal stresses. The steel layout and dimensions of the panels in the CA and CE series are shown in Fig. 1.

Figs. 2 and 3 are the test results of the shear stress - shear strain curves of panels CA3 and CE3 respectively. In Figs. 2 and 3, “C” means the cracking shear stress of panel; “YT” stands for the yielding of steel bars in the transverse direction; “YL” represents the yielding of steel bars in the longitudinal direction; “M” is the maximum shear stress.

The test results show that the effect of the steel grid orientation plays an important role on the shape of the post-yield hysteretic loops. “The panels of the CA series display a highly pinched shape in the hysteretic loops of the shear stress ~ shear strain curves. In contrast, the hysteretic loops of the panels of the CE are found to be robust, fat, well-rounded, and with no trace of the pinched shape” (Mansour [7]).



(a) Steel layout and dimensions of the panels in the CA-series ($\alpha_2 = 45^\circ$)



(b) Steel layout and dimensions of the panel in the CE-series ($\alpha_2 = 90^\circ$)

Fig. 1 Steel layout and dimensions of the panels in the CA and CE series (Dimensions are in mm)

The shear strains and shear stresses at critical points of CA and CE series are compared in Table. 1. That shows the specimens in CE series have greater shear ductility than those in the CA series. Since the tests on the CE series were forced to be terminated due to the limitation of the strokes in the testing system, the real value of the maximum shear strain and shear stress and ductility would be larger.

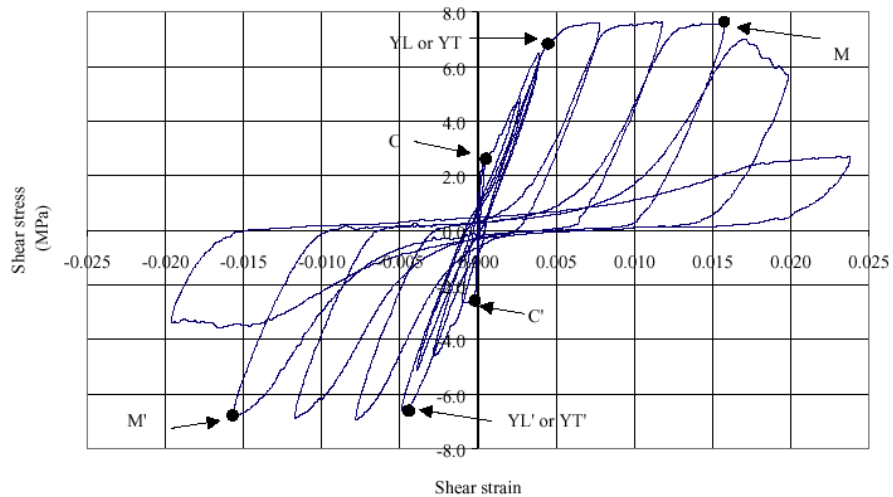


Fig. 2 Cyclic shear stress-strain curves of panels in the panel CA3

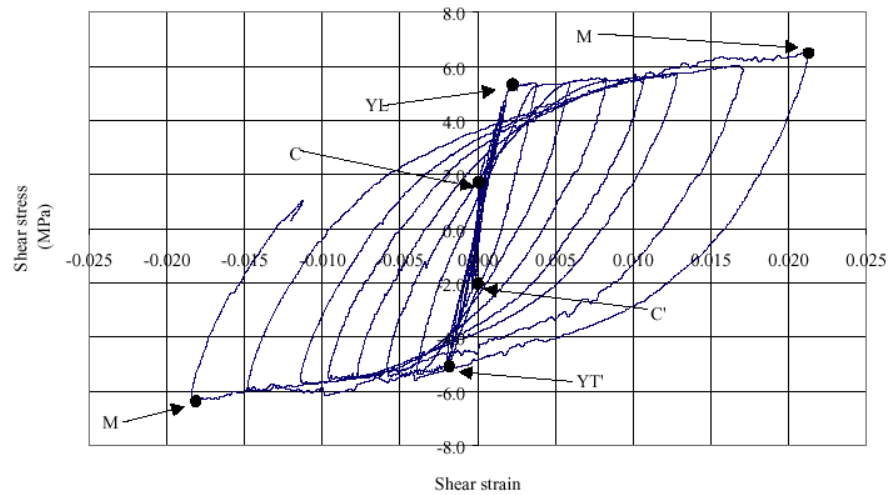


Fig. 3 Cyclic shear stress-strain curves of panels in the panel CE3

Table. 1 Shear strains and shear stresses at critical points of CA and CE series

Panel	ρ_l	ρ_t	Positive loading direction					Negative loading direction				
			γ_y	τ_y	γ_{max}	τ_{max}	μ	γ_y	τ_y	γ_{max}	τ_{max}	μ
CA2	0.0077	0.0077	0.0039	3.55	0.023	3.85	5.84	0.0040	3.50	0.0264	3.91	6.67
CA3	0.017	0.017	0.0045	6.70	0.0157	7.59	3.49	0.0048	6.61	0.0156	6.83	3.25
CA4	0.027	0.027	0.0057	10.2	0.0075	10.54	1.32	0.0056	10.1	0.0077	10.2	1.38
CE2	0.0054	0.0054	0.002	2.31	0.0125	2.73	6.25	0.0019	2.68	-0.019	3.6	10.11
CE3	0.012	0.012	0.0022	5.31	0.021	6.45	9.55	0.0020	5.10	-0.018	6.29	9.09
CE4	0.019	0.019	0.0019	8.11	0.0122	8.36	6.42	0.0023	7.60	0.0114	8.26	4.96

Unit of stress: Mpa; γ_y = yield shear strain; τ_y = yield shear stress; γ_{max} = shear strain corresponding to τ_{max} ; τ_{max} = maximum shear stress; μ = ductility = γ_{max} / γ_y .

TEST PROGRAM

Shake table tests

Two low-rise shear walls (STB, STN) were tested on a shake table that was subjected to a simulated earthquake ground motion. The height to width ratio of walls is 0.5. The height, length, and width of the designed shear walls for the shake table tests are 0.7 m, 1.4 m and 0.085 m, respectively. Boundary elements are provided on the two sides of specimen STB. In the walls of the two specimens, steel bars are provided in the directions of 45 degree to the horizontal that are close to the orientation of the principal direction of applied tensile stresses, as shown in Fig. 4.

Materials

Concrete

The concrete compressive strength of the shear walls and foundations are 16.58MPa and 30.16MPa, respectively.

Rebars

As shown in Fig. 4, No.2 bars are used in the stirrups of boundary elements of specimen STN. No.3 bars are used as the steel grids of the two walls, the stirrups of bottom foundations of the two walls, and the longitudinal bars of the boundary elements of specimen STN. No.5 bars are used as the longitudinal

bars of the boundary elements of specimen STB. No.7 bars are used in the top plate and the bottom foundations.

The yield and ultimate stresses of the used rebars are listed in Table. 2.

Table. 2 Yield and ultimate stress of rebars

	Yield stress	Ultimate stress
#2 Rebar	528 MPa	535 MPa
#3 Rebar	346 MPa	474 MPa
#5 Rebar	403 MPa	566 MPa
#7 Rebar	507 MPa	656 MPa

Structure

The height, length, and width for both walls STN and STB are 0.7 m, 1.4 m and 0.085 m, respectively. It should be noted that, in specimen STB, the end regions of the shear wall are provided with columns as boundary elements. The cross section of the columns is 120mm by 120mm and provided with longitudinal bars and stirrups. For specimen LN, the thickness of the wall is same along the length, and concealed columns with longitudinal bars and stirrups are provided at the ends of the wall. Fig. 4 indicates the dimensions and reinforcement of specimen STB and STN. The steel ratios in the perpendicular direction for specimens STB and STN are both 0.36%.

Instrumentation

The horizontal displacements of the walls were measured by LVDTs. The response acceleration of the walls was measured by accelerameters. In order to measure deformation in reinforcing bars, strain gauges were placed on the rebars in the walls. The locations of the strain gauges are indicated in Fig. 4.

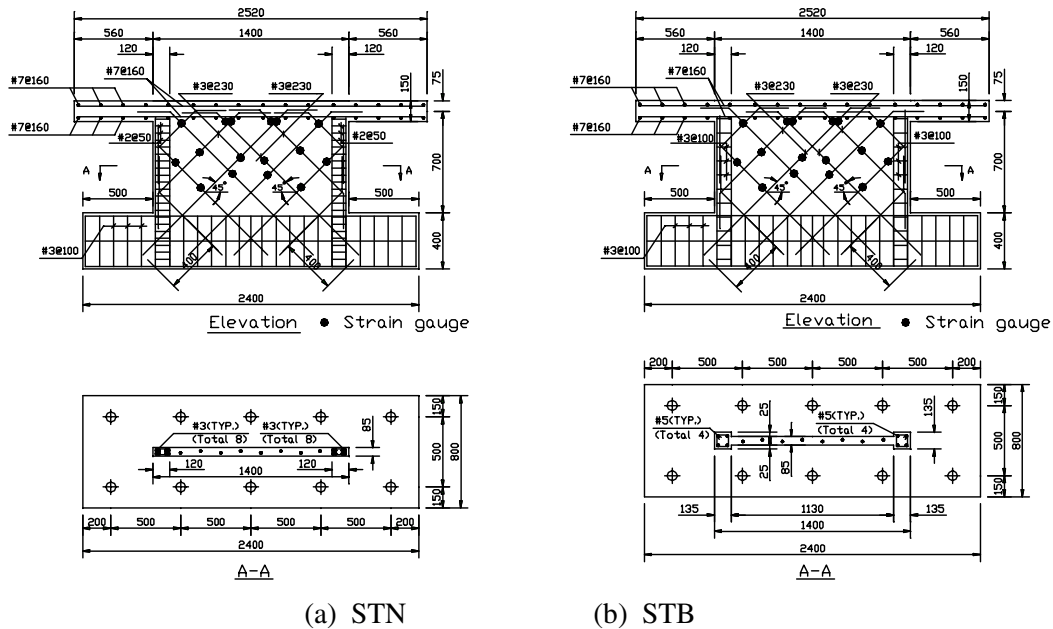


Fig. 4 Dimensions and reinforcement of specimens STN and STB

Test set-up and procedure

Fig.5 shows a photo of the test set-up of shake table tests. For specimen STN, a total mass of 13500 kg was put at the top and bottom of the top plate. For specimen STB, a total mass of 13500 kg was put at the top of the top plate in the first four runs of tests. A mass of 4500 kg was added to the top plate in the last two runs.

The tcu078Eji seismogram of the 1999 Taiwan earthquake was used as the ground motion acceleration. The normalized seismogram is shown in Fig. 6.



Fig. 5 Test set-up of shake table tests

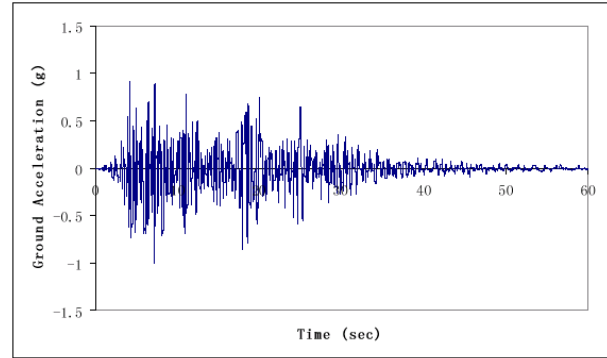


Fig. 6 Normalized tcu078Eji seismogram of the 1999 Taiwan earthquake

A summary of the test runs is included in Table. 3 and Table. 4 for specimens STN and STB, respectively. For specimen STB, 0.05g run was skipped because it is in the elastic response.

Table. 3 Test runs of specimen STN

Run number	PGA*	Remark
1	0.05g**	
2	0.4g**	
3	0.8g**	
4	1.2g**	Steel yielded
5	1.6g**	Failure

Note: * PGA = peak ground acceleration; **Mass = 13500 kg

Table. 4 Test runs of specimen STB

Run number	PGA*	Remark
1	0.4g**	
2	0.8g**	Steel yielded
3	1.2g**	
4	1.6g**	
5	1.2g***	
6	1.6g***	Failure

Note: * PGA = peak ground acceleration; **Mass = 13500 kg; ***Mass = 18000 kg

Reversed cyclic tests

Two low-rise shear walls (LB, LN) were tested under reversed cyclic horizontal loading. The height to width ratio of walls is 0.5. As shown in Fig. 7, steel bars are provided in the directions of 45 degree to the horizontal direction.

Materials

Concrete

The concrete compressive strength of the shear walls and foundations are 35.63MPa and 35.98MPa, respectively.

Rebars

As shown in Fig. 7, No.3 bars are used as the steel grids of the walls, the stirrups of boundary elements and the bottom foundations. No.7 bars are used as the longitudinal bars of the boundary

elements of specimen LB. The yield stress of No.3 bars is 329MPa. The yield strength of No.7 bars is 545MPa.

Structure

The height, length, and width for both walls LN and LB are 1.4 m, 2.8 m and 0.12 m, respectively. For the specimen LN, the thickness of the wall is same along the length, and concealed columns with longitudinal bars and stirrups are provided at the ends of the wall. In the specimen LB, the end regions of the shear wall are provided with columns with longitudinal bars and stirrups, and the cross section of the columns are 240mm by 240mm. Fig. 7 indicates the dimensions and reinforcement of specimen LN and LB. The steel ratios in the perpendicular direction for specimens LN and LB are 0.48%.

Instrumentation

The horizontal displacements of the walls were measured by LVDTs. In order to measure deformation in reinforcing bars, strain gauges were placed on the rebars in the walls.

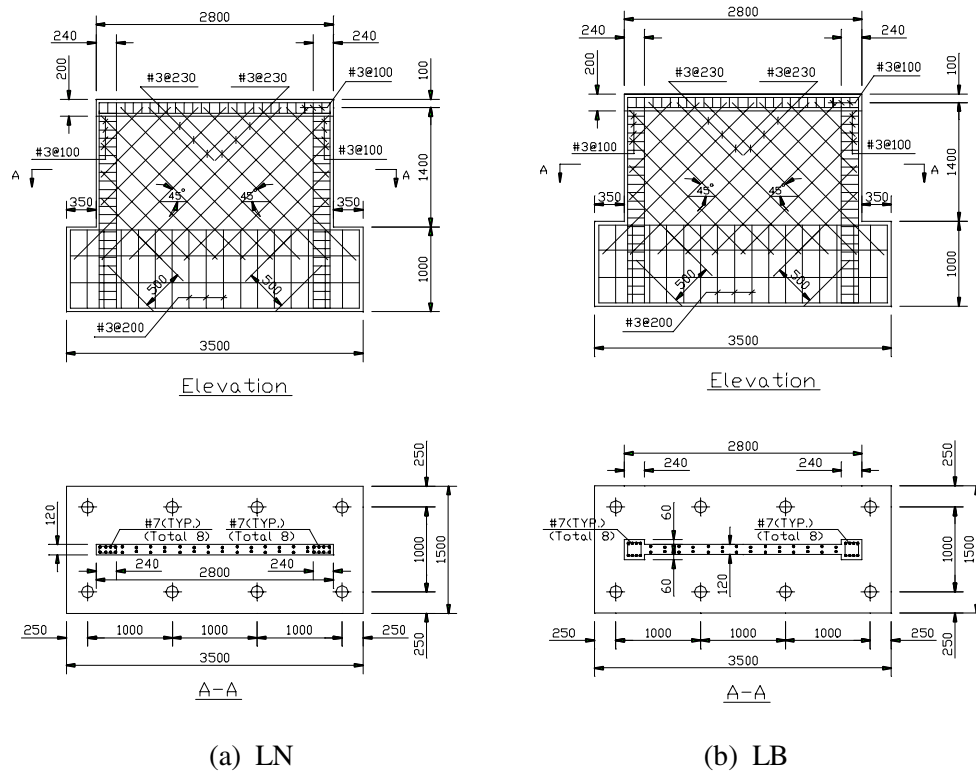


Fig. 7 Dimensions and reinforcement of specimens LN and LB

Test set-up and procedure

Fig.8 shows a photo of the test set-up for reversed cyclic tests. Reversed cyclic horizontal loadings are applied on the top of the shear wall. The test procedure is controlled by the horizontal displacement at the top of the wall. The scheme of the displacement control is shown in Fig.9.



Fig. 8 Test set-up of reversed cyclic test

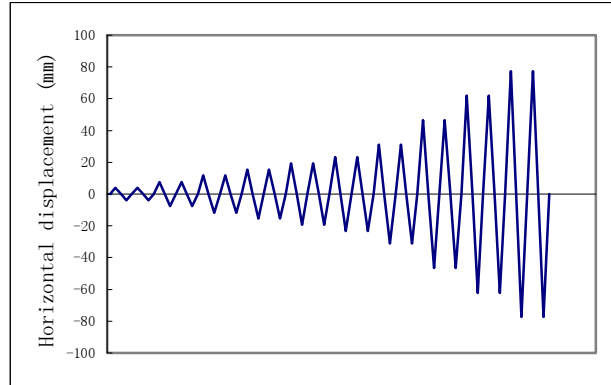


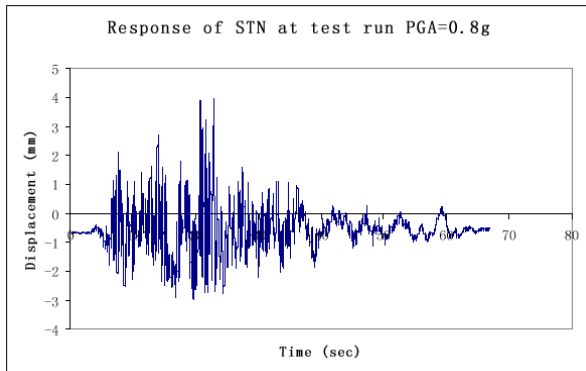
Fig. 9 Displacement control scheme of reversed cyclic tests

TEST RESULTS

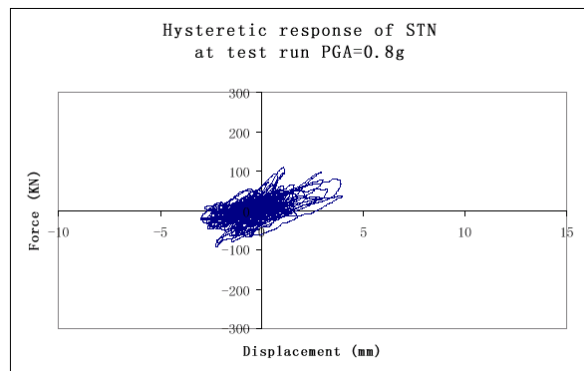
Shake table tests

Failure modes and hysteretic response

For specimen STN, the measurements from the strain gauges show that the first yield of steel bars occurred at the fourth run when the maximum ground acceleration equals to 1.2 g. The failure of the wall happened at the fifth run when the maximum ground acceleration equals to 1.6 g. The failure is caused by concrete crushing due to shear. The hysteretic response of the last three runs is shown in Fig. 10 to 12.



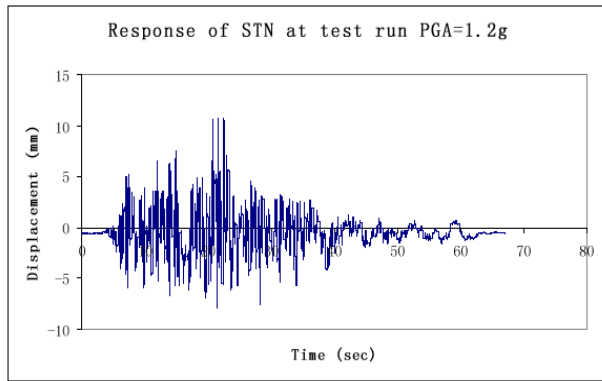
(a) Time history of response



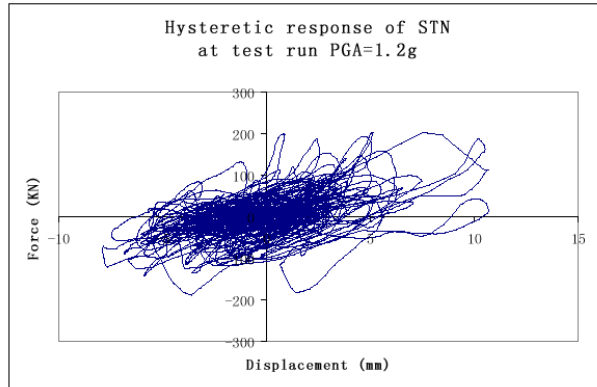
(b) Hysteretic response

Fig. 10 Hysteretic response of specimen STN at the third test run PGA = 0.8 g

By comparing the responses of the third, fourth and fifth runs, it shows that the maximum displacement and acceleration in each run increase progressively when the peak ground acceleration (PGA) of the input seismogram increases. The experimental dissipated energy is determined by integrating the areas bounded by all the hysteretic loops. The dissipated energy of the fourth run and the fifth run are much greater than the third run.

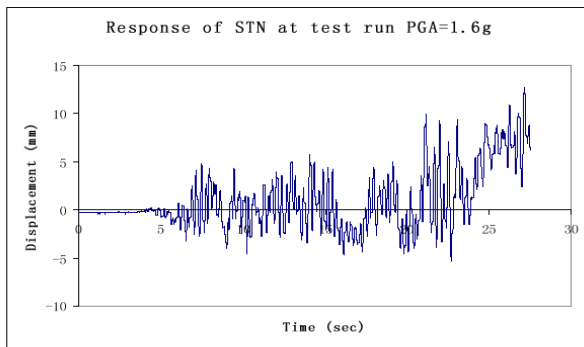


(a) Time history of response

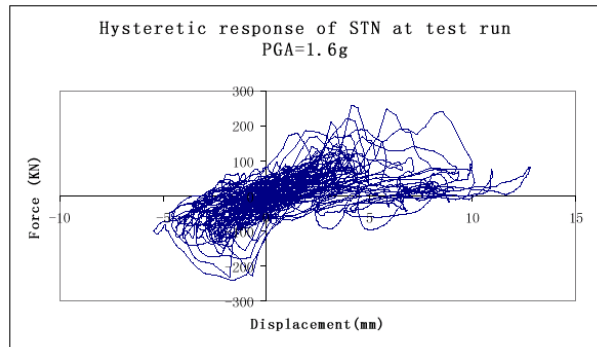


(b) Hysteretic response

Fig. 11 Hysteretic response of specimen STN at the fourth test run PGA = 1.2 g



(a) Time history of response

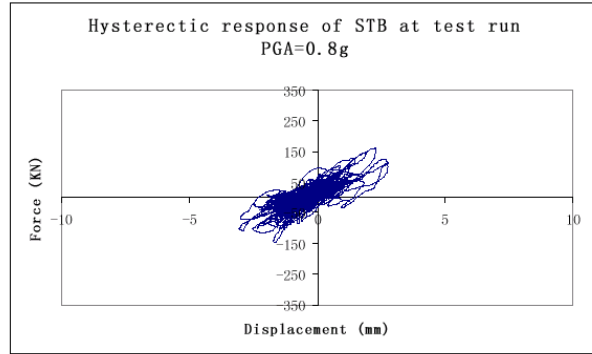
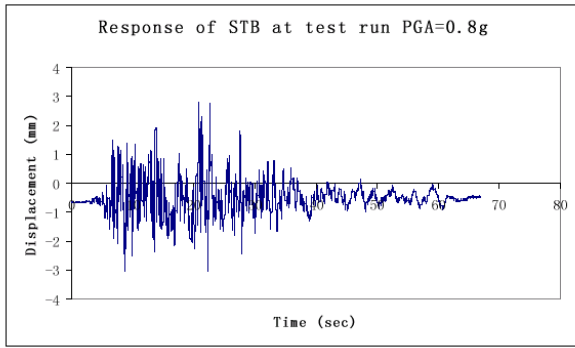


(b) Hysteretic response

Fig. 12 Hysteretic response of specimen STN at the fifth test run PGA = 1.6 g

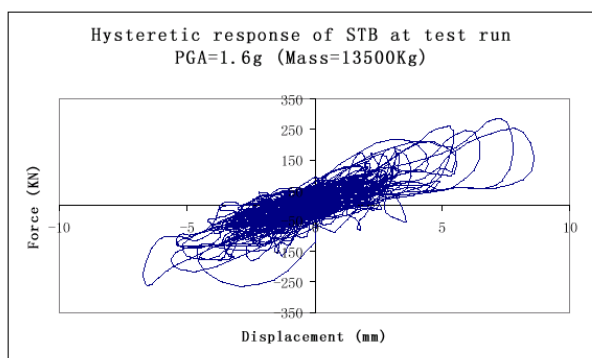
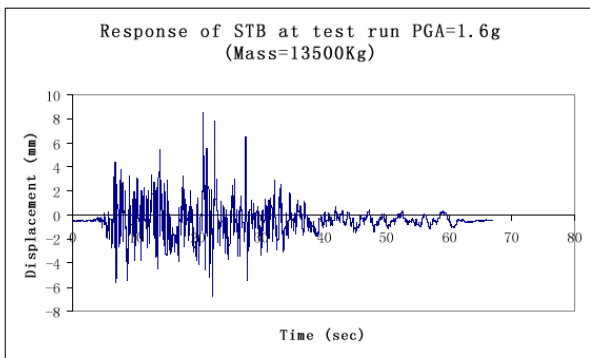
For specimen STB, the measurements from the strain gauges show that the first yield of the steel bars occurred at the second run when the maximum ground acceleration equals to 0.8 g. After the fourth run, specimen STB did not fail. A mass of 4500 kg was added to the top of the top plate. Another two runs (fifth and sixth runs) were performed, and specimen failed during the sixth run. Rocking of the top plate was observed during the last two runs that occurred due to the eccentricity of mass on the top plate after extra mass was added. Concrete crushing was found at the connection of the wall and top plate when the specimen failed. Shear wall did not exhibit an obvious failure. The hysteretic response of the second, fourth, and sixth run of specimen STB are shown in Fig. 13 to Fig. 15, respectively.

During the second, third, and fourth test runs, the maximum displacement and acceleration in each run increased progressively when the PGA of the input seismogram increases. In the fourth run, the mass on the top plate is 13500 Kg and the PGA is 1.6 g. Maximum input force = 13500 Kg X 1.6 g = 216 KN. At the fifth run, the PGA is 1.2 g, and the total mass is 18000 Kg after the extra mass was added. Maximum input force = 18000 Kg X 1.2 g = 216 KN. Because the maximum input force is same for the fourth and the fifth run, the response displacement and acceleration of the fourth run and the fifth run are very close. Similar to specimen STN, the dissipated energy of the test runs of specimen STB is increased progressively when the PGA of each run increases.



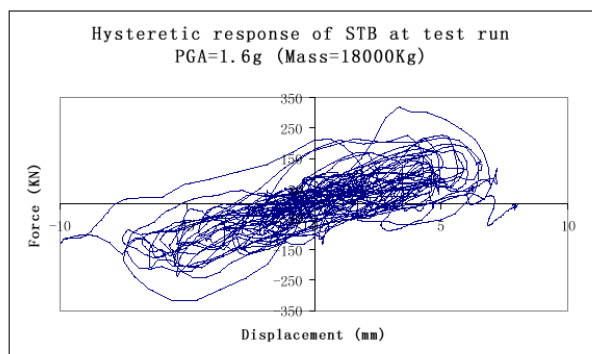
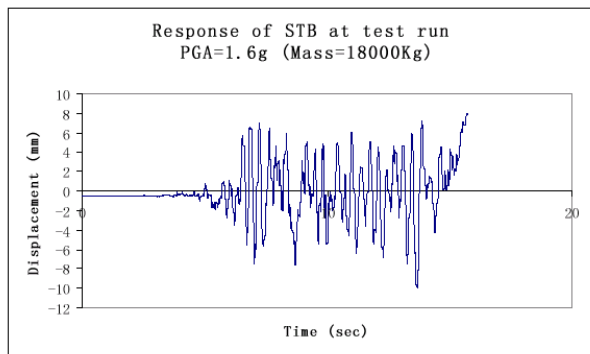
(a) Time history of response (b) Hysteretic response

Fig. 13 Hysteretic response of specimen STB at the second test run PGA=0.8g



(a) Time history of response (b) Hysteretic response

Fig. 14 Hysteretic response of specimen STB at the fourth test run PGA=1.6g (Mass=13500Kg)



(a) Time history of response (b) Hysteretic response

Fig. 15 Hysteretic response of specimen STB at the sixth test run PGA=1.6g (Mass=18000Kg)

Ductility and strength

The ductility and maximum shear force of shear walls STN and STB are shown in Table. 5. Test results show specimen STB has around 30% higher strength than STN, which may be caused by the boundary member elements of STB. Both of the shear walls have ductility greater than 7.0. The ductility of specimen STB may be larger if the test could be improved by eliminating the eccentricity created by the added top mass.

Table. 5 Ductility and maximum shear force of STN and STB

	Δ_y (mm)	Δ_m (mm)	Δ_u (mm)	μ	Maximum shear force(KN)
STN	0.895	4.45	8.53	9.53	256.5
STB	1.05	3.33	7.81	7.44	324.0

Reversed cyclic tests

Failure modes and hysteretic response

Figs.16 and 17 show the cracking patterns and failure mode of specimens LN and LB, respectively. The cracking of the concrete was drawn on the white painted faces of the specimens during the tests. During the tests, uniformly distributed cracks were observed in specimen LN and LB, and the crack orientations under reversed cyclic loading are nearly perpendicular and close to 45 degree direction. No failure at the boundary ends of the walls was found in specimens LN and LB during the tests. For specimen LN, the top beam failed first; then the concrete spalled in the interface between the top beam and the wall. It should be noted that the wall did not failed yet. For specimen LB, the length and width of the cracks developed during the reversed cyclic horizontal loading. Concrete crushing and rebars buckling were observed at the middle region of the wall.



Fig.16 Photo of specimen LN at failure stage



Fig.17 Photo of specimen LB at failure stage

The force-displacement relationship of specimens LN and LB are shown in Fig. 18 and Fig. 19, respectively. The hysteretic loops of the specimens LN and LB are found rounded and no obvious pinching effect is observed that is the typical phenomenon for low-rise conventional shear walls when rebars are provided in horizontal and vertical directions.

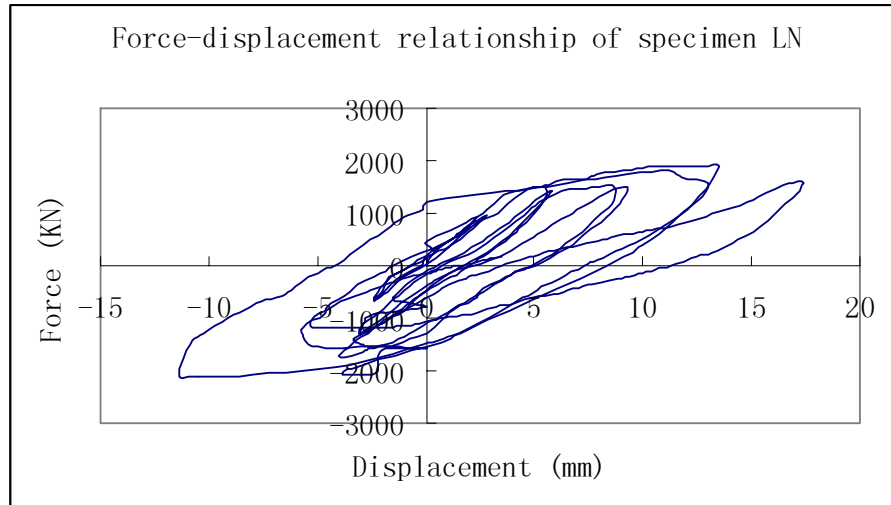


Fig. 18 Force-displacement of specimen LN

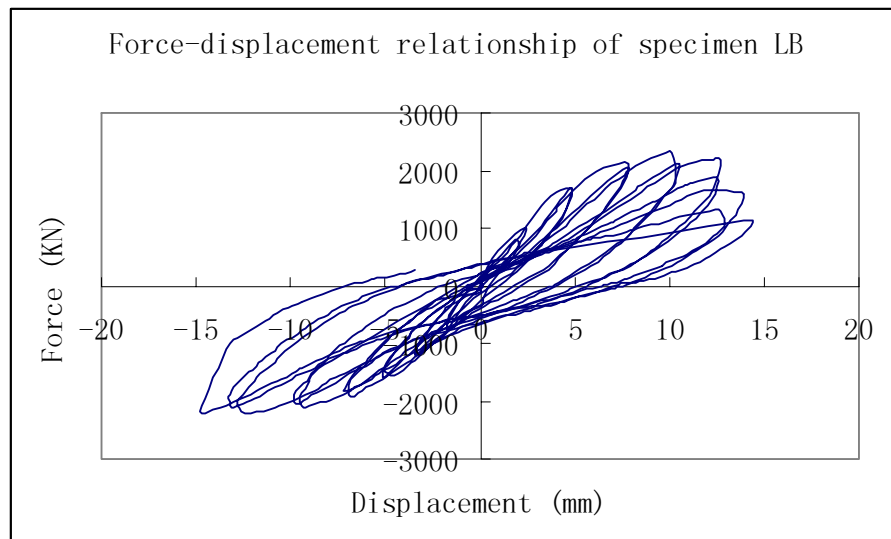


Fig.19 Force-displacement of specimen LB

Ductility and strength

The ductility and maximum shear force of specimens LN and LB are shown in Table.6. It is noted that the specimen LN failed due to the weak top beam and interface between the top beam and the wall, the strength and ductility of LN does not reflect the maximum capacity of the specimen. The strength and ductility would be increased if the top beam is strengthened.

Table.6 Ductility and maximum shear force of LN and LB

	Δ_y (mm)	Δ_m (mm)	Δ_u (mm)	μ	Maximum shear force(KN)
LN	3.81	11.40	17.40	4.57	2109
LB	2.90	10.13	14.78	5.10	2313

CONCLUSIONS

The shear walls tested in this study have greater ductility than that of conventional shear walls. Test results show that the high seismic performance of shear walls can be achieved when steel bars are provided in the direction of applied principal stresses.

REFERENCES

1. Cheng, F. Y. , Mertz, G. E., Sheu, M. S. and Ger, J. F. (1993). "Computed versus observed inelastic seismic low-rise RC shear walls." *Journal of Structural Engineering*, v 119, n 11, Nov, 1993, 3255-3275.
2. Colotti, V. (1993). "Shear behavior of RC structural walls." *Journal of Structural Engineering*, v 119, n 3, Mar, 1993, 728-746.
3. Eberhard, M. O. and Sozen, M.A. (1993). "Behavior-based method to determine design shear in earthquake-resistant walls." *Journal of Structural Engineering*, v 119, n 2, Feb, 1993, 619-640.
4. Elnashai, A. S., Pilakoutas, K. and Ambraseys, N. N. (1990). "Experimental behaviour of reinforced concrete walls under earthquake loading." *Earthquake Engineering & Structural Dynamics*, v 19, n 3, Apr, 1990, 389-407.
5. Farrar, C. R. and Baker, W. E. (1992). "Measuring the stiffness of concrete shear walls during dynamic tests." *Experimental Mechanics*, v 32, n 2, Jun, 1992, 179-183.
6. Lopes, M. S. (2001). "Experimental shear-dominated response of RC walls. Part I: Objectives, methodology and results." *Engineering Structures*, v 23, n 3, Mar, 2001, 229-239.
7. Mansour, M. (2001). "Behavior of Reinforced Concrete Membrane Elements under Cyclic Shear: Experiments to Theory." *PhD dissertation*, Department of Civil Engineering, University of Houston, August 2001.
8. Mansour, M., Lee, J. Y. and Hsu, T. T. C. (2001). "Constitutive Laws of Concrete and Steel Bars in Membrane Elements under Cyclic Loading." *Journal of Structural Engineering*, ASCE, Vol. 127, No. 12, Dec. 2001, 1402-1411.
9. Mo, Y. L. and Kuo, J. Y. (1998). "Experimental studies on low-rise structural walls." *Materials and Structures*, v 31, n 211, Aug-Sep, 1998, 465-472.
10. Mo, Y. L. and Lee, Y. C. (2000). "Shake table tests on small-scale low-rise structural walls with various sections." *Magazine of Concrete Research*, v 52, n 3, Jun, 2000, 177-184.
11. Pilakoutas, K. and Elnashai, A. S. (1995). "Cyclic behavior of reinforced concrete cantilever walls, Part II: discussions and theoretical comparisons." *ACI Structural Journal*, v 92, n 4, Jul-Aug, 1995, 425-434.
12. Sittipunt, C., Wood, S. L., Lukkunaprasit, P. and Pattararattanakul, P. (2001). "Cyclic behavior of reinforced concrete structural walls with diagonal web reinforcement." *ACI Structural Journal*, v 98, n 4, July/August, 2001, 554-562.
13. Tasnimi, A. A. (2000). "Strength and deformation of mid-rise shear walls under load reversal." *Engineering Structures*, v 22, n 4, Apr, 2000, 311-322.
14. Wood, S. L. (1990). "Shear strength of low-rise reinforced concrete walls." *ACI Structural Journal* v 87, n 1, Jan-Feb, 1990, 99-107.